

Onboard Model-based Prediction of Tram Braking Distance^{*}

Loi Do^{*} Ivo Herman^{**} Zdeněk Hurák^{***}

^{*} Faculty of Electrical Engineering, Czech Technical University in Prague, CZ (e-mail: doloi@fel.cvut.cz).

^{**} Herman Electronics, Brno, CZ (e-mail: ivo.herman@herman.cz).

^{***} Faculty of Electrical Engineering, Czech Technical University in Prague, CZ (e-mail: hurak@fel.cvut.cz)

Abstract: In this paper, we document a design of a computational method for an onboard prediction of a braking distance for a city rail vehicle—a tram. The method is based on an onboard simulation of tram braking dynamics. Inputs to this simulation are the data from a digital map and the estimated (current) position and speed, which are, in turn, estimated by combining a mathematical model of dynamics of a tram with the measurements from a GNSS/GPS receiver, an accelerometer and the data from a digital map. Experiments with real trams verify the functionality, but reliable identification of the key physical parameters turns out critically important. The proposed method provides the core functionality for a collision avoidance system based on vehicle-to-vehicle (V2V) communication.

Keywords: Automatic control, optimization, real-time operations in transportation, Simulation, Braking distance prediction, Rail transport, Mathematical modelling

1. INTRODUCTION

1.1 Motivation, short description

In this paper, we present a computational method for prediction of a tram braking distance based on an onboard simulation of a mathematical model of tram braking dynamics. The proposed algorithm runs onboard the tram. It combines in real time the outputs from the mathematical model of longitudinal dynamics of the tram with the signals provided by a GNSS/GPS receiver, an inertial measurement unit (IMU), and the data read from a digital map. The parameters of the model of dynamics of the tram can be partially determined from the technical specifications provided by the producer and partially extracted from data measured using onboard sensors during experiments (grey box identification). Although in this paper, we consider one particular tram brand and type, the proposed procedure can be applied to any (light) rail vehicle.

The motivation for such development is the disturbingly high number of collisions of trams with other trams, other vehicles, and even pedestrians¹. Different collision scenarios call for different approaches to their solutions. In the research described in this paper, we restrict ourselves to the development of collision avoidance between vehicles. In particular, we consider tram-to-tram collisions. The reason for considering collisions between trams is that both participants in the (potential) collision are operated by a single organization/company, which makes coordi-

nated collision avoidance schemes (almost) immediately realizable. The key technology for such coordination is wireless vehicle-to-vehicle (V2V) communication, through which the trams could exchange their position and speed estimates and predictions, thus truly distributed estimation/predictions could be realized. One of the essential components of such a collision avoidance system is a reliable prediction of tram braking distance, which we cover in this paper.

1.2 State of the art

In general, real time prediction of braking distance (or motion in general) of rail vehicles plays an important role in *safety* application (Lehner et al., 2009), (Gu et al., 2013), (Wu et al., 2018) or *energy optimization* (Lu et al., 2016), (Keskin and Karamancioglu, 2016). For safety applications involving suburban or freight trains, the prediction of braking distance need not be accurate due to relatively large gap distance (to the next train) and approximately constant parameters of the train dynamics. Simple braking distance prediction models based only on constant parameters of heavy-weight trains their current speed and track characteristics have been published (IEEE, 2009).

In cities with a dense tram network, however, the distance gap between two (rail or road) vehicles could go down to a few meters (stopping at tram stops or traffic lights), resulting in a higher probability of collisions. This imposes higher requirements on the accuracy of related onboard estimations and predictions, which are, in turn, conditioned by the accurately identified physical parameters. The parameters are mainly the weight of the vehicle, which is given by the actual number of passengers (the total weight of the tram can be some 50 % higher from an

^{*} The research was funded by Technology Agency of the Czech Republic within the program Epsilon, the project TH03010155.

¹ Prague Public Transit, Co. Inc. has been registering well above one thousand collisions every year.

empty tram), the coefficients characterizing the adhesion conditions (given by humidity, temperature) and slope of the track (tramways). Not many works in the literature seem to be systematically addressing these issues.

One component of the full collision avoidance system is an estimator of the (distance) gap, that is, the distance between the rear bumper of the leading vehicle and the front bumper of the following vehicle. One class of these estimators is based on vision-based techniques (Mukhtar et al., 2015). An alternative followed in the broader project, within which we write this paper, is to use the V2V communication (Xiang et al., 2014), (Abboud et al., 2016) between the two vehicles and, effectively, realize an estimator of the distance gap in a distributed manner. Nonetheless, in this paper, we do not elaborate further on this topic of the distance gap estimation.

1.3 Outline of the paper

This paper is structured as follows. In Sec. 2, we give some background information about the Tatra T3 tram. We also describe the instrumentation used for onboard measurements. Then in Sec. 3 we describe the model of dynamics with the values of the physical parameters identified from real data obtained in experiments with trams and document the verification of the model. In Sec. 4, we explain the use of the model for prediction of braking distance and describe in more detail estimation of the position and the speed of a tram. We also compare the proposed method with a simple equation-based braking distance prediction method. Lastly, we give a conclusion in Sec. 5.

2. EXPERIMENTAL SETUP

2.1 Tatra T3 tram

We focus on developing a model of dynamics of the Tatra T3 tram partially parameterized by data acquired onboard a tram during experiments. With nearly 14 thousand produced trams during the period from 1960 to 1989, the T3 tram is one of the most produced tram cars in the world (Mara, 2001). In the Czech Republic, T3 trams (in several modernized versions) are still used nowadays and form a significant portion of public transport tram fleets in many cities. Proportions of the tram and parameters relevant for the modeling are listed in Tab. 1 (Linert et al., 2005).

Table 1. Parameters of the T3 tram.

Parameter	Notation	Value
Curb weight	-	≈ 16 500 kg
Gross weight	-	≈ 27 500 kg
Body length	-	14 000 mm
Body height	-	3060 mm
Body width	-	1440 mm
Wheel radius	r	325 mm
Wheel mass	m_w	195 kg
Maximum speed	-	65 km h ⁻¹
Total power of motors	P_{\max}	4 × 44 kW

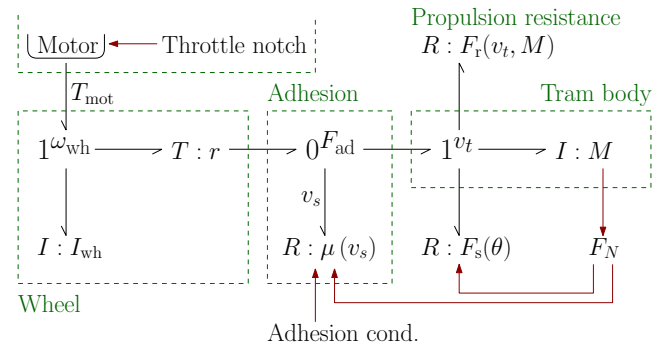


Fig. 1. Bond graph of the longitudinal motion dynamics.

2.2 Instrumentation

The instrumentation in the T3 tram measures only a few values, for instance, tram speed (computed from a wheel speed) or applied current to motor. We, however, could not directly read these data during the experiments due to the lack of the CAN bus in the tram. We, therefore, used external instrumentation to collect the measurements for the model identification. We used GNSS receiver *NEO-M8P* by *U-blox* to measure the position and the speed of the tram and inertial measurement unit (IMU) *ADIS16465-1BMLZ* by *Analog devices* to measure the acceleration. We used ready-to-use application/evaluation boards from the manufacturer to directly read the measurements from the sensors. We set the sampling frequency of the GNSS/GPS receiver to 1 Hz and the sampling frequency of the IMU to 2 kHz. We aligned the x-axis of IMU with the direction of the longitudinal motion of the tram.

3. MODEL OF DYNAMICS

3.1 Identification of a model

For the prediction of braking distance, it is sufficient to use the quarter model of dynamics describing only the longitudinal motion of a tram (Sadr et al., 2016). The quarter model of dynamics is given by equations:

$$J_{wh}\dot{\omega}_{wh} = (T_{mot} - rF_{ad}) , \quad (1a)$$

$$M\dot{v}_t = (F_{ad} - F_r - F_s) , \quad (1b)$$

where ω_{wh} is the angular speed of the wheel, J_{wh} is a moment of inertia of the wheel, T_{mot} is torque given from the motors, r is the radius of a wheel, F_{ad} is adhesion force, v_t is the longitudinal speed of the tram, M is the total weight of the tram, F_r and F_s are resistive forces. This model can be also described by a *bond graph* (Paynter, 1960) displayed in Fig. 1. Approximating the wheel as a homogeneous disk, we can write its moment of inertia as:

$$J_{wh} = 0.5m_w r^2 . \quad (2)$$

The total weight of the tram M is a sum of the curb weight and weight of passengers in the tram. The torque T_{mot} generated by the motors is proportional to the notch (position) of the control throttle. In the T3, the throttle control has in total 15 notches: seven notches for acceleration, seven notches for deceleration, and one notch for idle. We identified the traction characteristics experimentally as:

$$\tilde{T}_{\text{mot}}(p) = \begin{cases} K_p p & \text{for } p \geq 0 \text{ and } T_{\text{mot}}\omega_{\text{wh}} < P_{\text{max}} , \\ P_{\text{max}}/\omega_{\text{wh}} & \text{for } p \geq 0 \text{ and } T_{\text{mot}}\omega_{\text{wh}} \geq P_{\text{max}} , \\ K_n p & \text{for } p < 0 , \end{cases} \quad (3)$$

where $p \in \{-7, -6, \dots, 0, \dots, 6, 7\}$ is the notch, $K_p = 1449$ and $K_n = 1176$ are constants of proportionality which were set to match experimentally measured maximal and minimal acceleration at the highest and lowest notch, respectively. Due to the electromechanical properties of T3 tram braking traction, the braking torque is not restricted by the P_{max} . Also, we model the dynamics of the change of \tilde{T}_{mot} as a first-order system (with unit steady state gain and time constant $\tau = 1/3$ s), giving the resulting value of the torque:

$$\dot{T}_{\text{mot}} = 3 \left(\tilde{T}_{\text{mot}}(p) - T_{\text{mot}} \right) . \quad (4)$$

The adhesion force F_{ad} accounts for the transfer of wheel speed into the longitudinal motion of the tram body. A physical explanation of the adhesion is given in Park et al. (2008). In general, the adhesion force F_{ad} is computed as a sum of adhesion force given by each traction wheel, and the adhesion force is proportional to the wheel load. However, since all wheels of T3 tram are connected to the traction motors and by assuming the uniform distribution of the tram weight on each wheel, we can directly write:

$$F_{\text{ad}} = \mu(v_s)F_N , \quad (5a)$$

$$F_N = Mg , \quad (5b)$$

$$v_s = r\omega_{\text{wh}} - v_t , \quad (5c)$$

$$\mu(v_s) = c_a \exp(-a_a v_s) - d_a \exp(-b_a v_s) , \quad (5d)$$

where g is the gravitational acceleration. Parameters a_a , b_a , c_a and d_a vary on track conditions (Takaoka and Kawamura, 2000).

Propulsion resistance F_r of rail vehicles (sum of rolling and air resistance) is typically calculated using an empirical equation in a form (Hay, 1982):

$$F_r(v_t) = A + Bv_t + Cv_t^2 , \quad (6)$$

where A , B and C are coefficients giving the dependence of propulsion resistance on characteristics of the rail vehicle such as weight, number of axles or front surface cross-sectional area. To identify coefficients in Eq. (6) we first

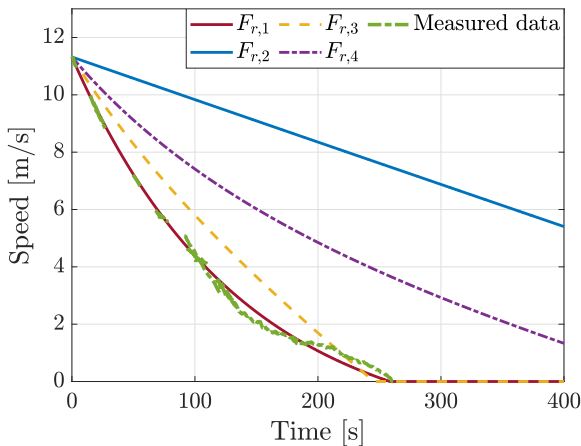


Fig. 2. Comparison of identified parameters for propulsion resistance and parameters from the literature.

gather all measurements from experiments during which the tram decelerate only due to propulsion resistance (idle notch), see Fig. 2 (*Measured data*). Note that we could not obtain longer continuous decay from higher speeds due to the restriction of the test track. We can simulate the model and set the same conditions as in the experiments to find appropriate coefficients. The weight of the tram during experiments was 17 000 kg (estimated from a number of people in the tram during the experiment). Since trams usually operate at lower speeds than other trains, we simplify the identification of Eq. (6) by neglecting quadratic dependence on v_t , thus setting $C = 0$. The identified propulsion resistance equation is:

$$F_{r,1}(v_t, M) = 0.0147M + 125.83v_t . \quad (7)$$

The reason why we do not use coefficients of Eq. (6) from the literature is that they are usually designed for rail vehicles which have significantly higher weight and also operate at higher speeds than trams. For instance, using the following equations from the literature evaluated for the T3 tram yields:

$$F_{r,2}(v_t, M) = 0.0147M + 2.18 \times 10^{-6} Mv_t^2 , \quad (8a)$$

$$F_{r,3}(v_t, M) = 520 + 0.0065M + 3.6v_t + 3.8880v_t^2 , \quad (8b)$$

$$F_{r,4}(v_t, M) = 1.839\sqrt{M} + 0.0036Mv_t + 4.329v_t^2 . \quad (8c)$$

Propulsion resistance $F_{r,2}$ was designed for passenger train on bogies (Iwnicki, 2006), $F_{r,3}$ for electric locomotive and $F_{r,4}$ for suburban electric multiple unit train (Rochard and Schmid, 2000). See the comparison in Fig. 2. We can see that the speed decay when using any of Eq. (8) does not match with the measurements.

Lastly, in addition to propulsion resistance, the motion of a tram is also affected by the slope θ (longitudinal inclination) of track:

$$F_s(\theta) = F_N \sin \theta . \quad (9)$$

Slope θ is positive for ascent and negative for the descent.

3.2 Verification of a model

To verify the model output with experimentally obtained data, we first reduce the noise and bias in the measured signal from the accelerometer. The longitudinal acceleration of rail vehicles is usually characterized by low-frequency signal (Heirich et al., 2011), whereas noise in the measurements is mainly caused by high-frequency vibrations on-board of a tram and sensor noise. Therefore, to remove the noise, we used the low-pass filter with the cut-off frequency 2 Hz. We verify the model by setting the same sequence of the throttle notch in the simulation, as in real experiment for two scenarios and compare the measured and simulated acceleration, speed, and total traveled distance.

In the scenario in Fig. 3, the driver was instructed to set the maximal acceleration for a certain amount of time and then set the maximal deceleration. We can see, that around time 5 s, $T_{\text{mot}}\omega_{\text{wh}} \geq P_{\text{max}}$ which results in decline of T_{mot} and thus decline in the acceleration. The total actual and simulated traveled distance during the experiment is 217 m and 207 m, respectively. The scenario in Fig. 4 has a more complicated sequence of throttle notches. The total actual and simulated traveled distance during this scenario is 158 m and 164 m, respectively. We can see that the modeled dynamics of the acceleration and

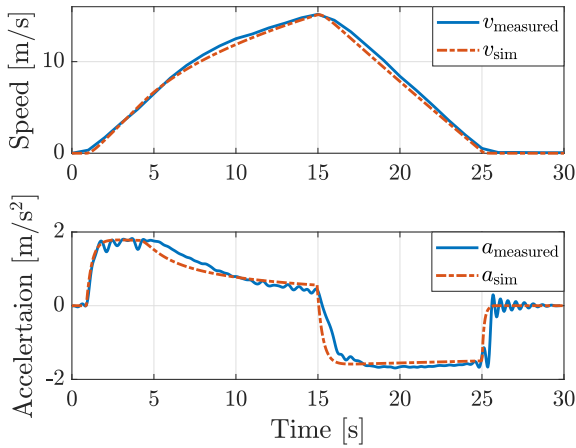


Fig. 3. Comparison of the model output and real measurements for the given sequence of throttle notches: maximal and minimal acceleration.

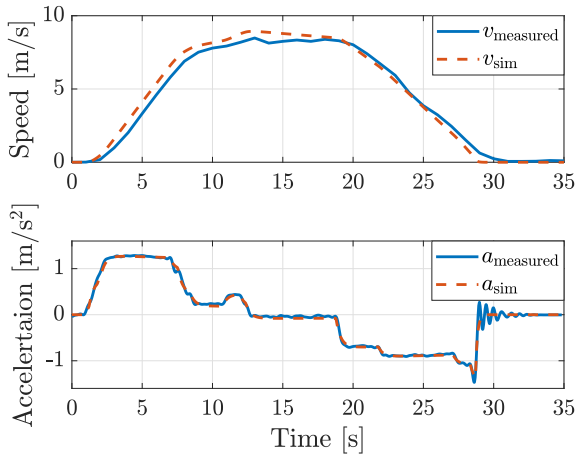


Fig. 4. Comparison of the model output and real measurements for the given sequence of throttle notches.

the speed is similar to the experimental data. Note that the discrepancies in total simulated and actual traveled distances (for both scenarios) are caused by a small error in generated acceleration, which is then integrated twice.

In both scenarios, the tram body at the moment of the stop exhibits oscillation due to the mechanics in the bogies. This effect is not incorporated into the model since it does not affect the braking distance.

We will conduct another verification experiments with varying conditions (different track, adhesion conditions, and a total weight M of the tram) by the end of the year 2019.

4. BRAKING DISTANCE PREDICTION

Using the model of dynamics developed in Sec. 3, the braking distance can be predicted onboard a tram as follows. First, the speed of the tram \tilde{v}_t is measured (or estimated) and used to set the initial conditions of the simulation: $v_t(0) = \tilde{v}_t$, $\omega_{wh}(0) = \tilde{v}_t/r$. The speed \tilde{v}_t can be estimated, for instance, by fusing measurements from GNSS/GPS receiver, IMU (Bar-Shalom et al., 2008),

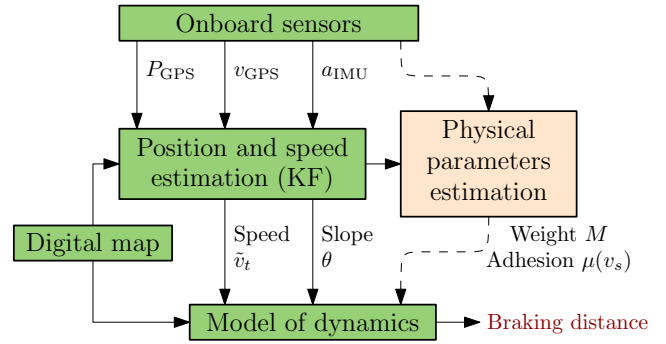


Fig. 5. Functionality of the proposed method for braking distance prediction. The estimation of the physical parameters is not covered in this paper.

or from the wheel speed (Ararat and Söylemez, 2017). The model of dynamics is then simulated with a selected notch ($p \leq 0$). Finally, the braking distance is obtained as the total traveled distance (time integration of v_t) from the start of the simulation until the simulated speed v_t is zero. Since the simulation of the proposed model is not computationally intensive, the simulation can be run periodically in real time onboard a tram, for instance, synchronously with the measurement or estimation of the speed v_t .

Furthermore, to get correct results, all following time varying physical parameters need to be estimated:

- Adhesion conditions: Estimation of the adhesion conditions (coefficients of $\mu(v_s)$) is well covered by various methods (Sadr et al., 2016), (Pichlik and Zdenek, 2018).
- Slope: The slope θ of the track can be retrieved from known absolute position and the data from digital map of the track or estimated from inertial measurements.
- Weight: The weight M could be estimated, for instance, from number of passengers in the tram counted by sensors at the tram entrances.

In the work which we present in this paper, we extensively focused only on the estimation of the absolute position (provides information of the slope θ) and the longitudinal speed using Kalman Filter (KF). We assume that the total weight and the adhesion conditions are known for the braking distance prediction. Functionality of the proposed method is depicted in Fig. 5.

4.1 Position and speed estimation

To estimate the absolute position and the longitudinal speed of a tram, we propose to use discrete-time linear KF with measurements from GNSS/GPS receiver (position P_{GPS} and speed v_{GPS}), IMU (longitudinal acceleration a_{IMU}), and data from the digital map of the track. We assume that the digital map provides geographic localization and value of the slope θ of each position of the track. The proposed estimation method is motivated by available sensor measurements onboard a T3 tram in our research.

Since the motion of a tram is restricted onto the track and the absolute position can be retrieved from the position on the track and digital map of the track, it is sufficient

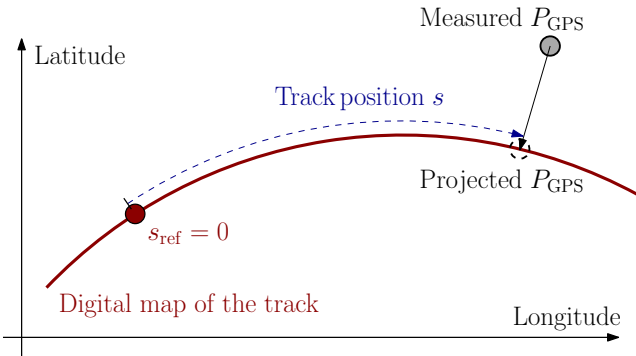


Fig. 6. Illustration of projection of a measured point x_{GPS} .

to estimate only the longitudinal dynamics of a tram. Let $x_k = [s_k, v_k, a_k]^T$ be a state vector of the track position, the speed, and the acceleration, respectively, at time instance k . With no information of input, we can describe time propagation of the state x_k using discrete-time constant acceleration model:

$$x_{k+1} = F_k x_k = \begin{bmatrix} 1 & \Delta t & 0.5\Delta t^2 \\ 0 & 1 & \Delta t \\ 0 & 0 & 1 \end{bmatrix} x_k \quad (10)$$

where Δt is sample time. Using the digital map, we can transform the measured geographic coordinates P_{GPS} into the track position s by the orthogonal projection of the P_{GPS} onto the track. The track position s is then given as a distance from a selected reference point s_{ref} on the track, see Fig. 6 for an illustration. Thus, the data from GNSS/GPS receiver directly serve as measurements of the track position s , and we can write the output equation of the model as:

$$y_k = H_k x_k = \begin{bmatrix} 1 & 0 & 0 \\ 0 & 1 & 0 \\ 0 & 0 & 1 \end{bmatrix} x_k \quad (11)$$

The matrices F_k and H_k defined by equations (10) and (11) can then be used in the standard linear KF algorithm. Also, suitable covariance matrices Q_k and R_k of process noise and measurement noise, respectively, should be selected according to the precision of used sensors.

4.2 Comparison of braking distance prediction methods

We now compare the proposed method for braking distance (model-based) prediction with the prediction using an equation (equation-based) derived from simple kinematics:

$$d_{br} = 0.5v_t^2 a_{dec}^{-1}, \quad (12)$$

where d_{br} is calculated braking distance and a_{dec} is selected braking deceleration. Such calculation of braking distance for rail vehicles has been published (IEEE, 2009) and used in several works (Lu et al., 2016), (Wu et al., 2018) due to its simplicity.

To get comparable results from equation-based and model-based methods, we set maximal deceleration of equation-based prediction (12) to $a_{dec} = 1.55 \text{ m s}^{-2}$ which approximately corresponds to maximal measured deceleration of empty tram with zero slope and dry adhesion conditions. We set such physical parameters in the simulation denoted as No. 1, see Fig. 7. We can see that the equation-based model gives in general lower braking distance (at 15 m s^{-1}

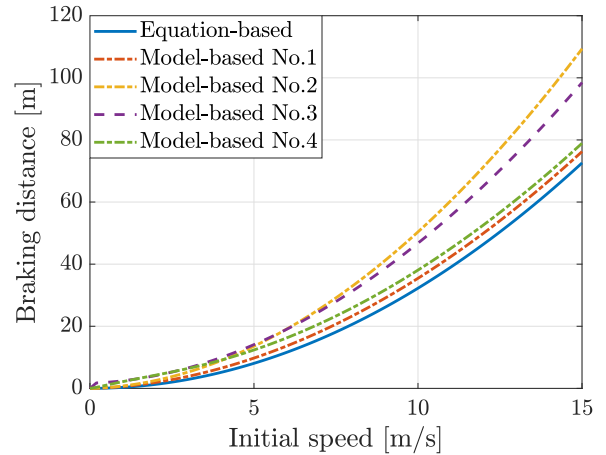


Fig. 7. Comparison of equation-based and model-based prediction of braking distance.

Table 2. Simulation parameters.

Sim. No.	Notch p	M [kg]	Slope θ [rad]	Adh. cond.
1	-7	17 000	0	Dry
2	-7	25 000	0	Dry
3	-7	17 000	-0.035	Dry
4	-7	17 000	0	Wet

lower by $\approx 4 \text{ m}$). The difference is mainly to the fact that model-based calculation, unlike the equation-based calculation, takes into account also the limited dynamics of deceleration.

For illustration, we also simulate the model with various parameters, see Tab. 2. Adhesion coefficients $[a_a, b_a, c_a, d_a]$ for dry conditions are: $[0.54, 1.2, 1, 1]$ and for wet conditions: $[0.05, 0.5, 0.08, 0.08]$ (Takaoka and Kawamura, 2000). From simulation No. 2, we can observe that even though a higher weight causes higher propulsion resistance, it also decreases maximal braking effort, which results in significantly higher braking distance. Braking distance is also significantly affected by the relatively small (negative) slope, as we can see from simulation No. 3. Simulation No. 4 shows that worse adhesion conditions have a higher effect on the braking distance at lower speeds ($\approx 5 \text{ m s}^{-1}$).

5. CONCLUSION AND FUTURE RESEARCH

In this paper, we presented a method for prediction of tram braking distance based on real time simulation of a model of dynamics of a tram. The braking distance prediction algorithm runs onboard a tram, taking as the inputs estimated longitudinal speed of a tram and key time-varying physical parameters affecting the braking distance such as the total weight of the tram, adhesion conditions, or the slope of the track. We have shown, through various simulations, that predicted braking distance significantly depends on values of the physical parameters. For safety applications such as collision avoidance, which is the ultimate goal of this research, the accurate prediction of braking distance is crucial for the correct detection of imminent collisions.

Besides the safety applications, within which we have written this paper, the model can be used in other applications

such as energy optimization or slip control. As a model of dynamics, we used a quarter model for a rail vehicle. We identified the parameters of the model partially from the literature and partially from the data measured using on-board sensors during real experiments. Also, by comparing the simulations of the model with real experiments, we verified its correctness. Another verification experiments with different physical parameters will be done by the end of the year 2019. The implemented model in Matlab and Simulink is downloadable at <https://www.mathworks.com/matlabcentral/fileexchange/73391>.

ACKNOWLEDGEMENTS

Significant help from Vít Obrusník with conducting the experiments is acknowledged. We would also like to express our gratitude to the engineers from Ostrava Public Transit Co. Inc. (Dopravní podnik Ostrava, a.s.) for enabling the experiments with trams.

REFERENCES

- Abboud, K., Omar, H.A., and Zhuang, W. (2016). Interworking of DSRC and Cellular Network Technologies for V2X Communications: A Survey. *IEEE Transactions on Vehicular Technology*, 65(12), 9457–9470. doi:10.1109/TVT.2016.2591558.
- Ararat, Ö. and Söylemez, M.T. (2017). Robust Velocity Estimation for Railway Vehicles. *IFAC-PapersOnLine*, 50(1), 5961–5966. doi:10.1016/j.ifacol.2017.08.1256.
- Bar-Shalom, Y., Li, X.R., and Kirubarajan, T. (2008). *Estimation with Applications to Tracking and Navigation: Theory Algorithms and Software*. Wiley-Interscience, 1st edition.
- Gu, Q., Zuo, H., Su, R., Zhang, K., and Xu, H. (2013). A Wireless Subway Collision Avoidance System Based on Zigbee Networks. *Journal of Communications*, 8(9), 561–565. doi:10.12720/jcm.8.9.561-565. URL <http://www.jcm.us/index.php?m=content&c=index&a=show&catid=121&id=574>.
- Hay, W.W. (1982). *Railroad Engineering*. Wiley, New York, 2nd edition.
- Heirich, O., Lehner, A., Robertson, P., and Strang, T. (2011). Measurement and analysis of train motion and railway track characteristics with inertial sensors. In *2011 14th International IEEE Conference on Intelligent Transportation Systems (ITSC)*, 1995–2000. doi:10.1109/ITSC.2011.6082908.
- IEEE (2009). IEEE Guide for the Calculation of Braking Distances for Rail Transit Vehicles. *IEEE Std 1698-2009*, C1–31. doi:10.1109/IEEESTD.2009.5332051.
- Iwnicki, S. (2006). *Handbook of Railway Vehicle Dynamics*. CRC Press. doi:10.1201/9781420004892.
- Keskin, K. and Karamancioglu, A. (2016). Energy Efficient Motion Control for a Light Rail Vehicle Using The Big Bang Big Crunch Algorithm. *IFAC-PapersOnLine*, 49(3), 442–446. doi:10.1016/j.ifacol.2016.07.824.
- Lehner, A., De Ponte Müller, F., Strang, T., and Rico García, C. (2009). Reliable vehicle-autarkic collision detection for railbound transportation. In *Proceedings of ITS 2009*. Stockholm, Sweden. URL <http://elib.dlr.de/60056/>.
- Linert, S., Fojtík, P., and Mahel, I. (2005). *Kolejová vozidla pražské městské hromadné dopravy*. Praha: Dopravní podnik hl. m. Prahy.
- Lu, S., Wang, M.Q., Weston, P., Chen, S., and Yang, J. (2016). Partial Train Speed Trajectory Optimization Using Mixed-Integer Linear Programming. *IEEE Transactions on Intelligent Transportation Systems*, 17(10), 2911–2920. doi:10.1109/TITS.2016.2535399.
- Mara, R. (2001). *Tatra T3 1960-2000 : 40 let tramvají Tatra T3*. K-Report.
- Mukhtar, A., Xia, L., and Tang, T.B. (2015). Vehicle Detection Techniques for Collision Avoidance Systems: A Review - IEEE Journals & Magazine. doi:10.1109/TITS.2015.2409109.
- Park, S.H., Kim, J.S., Choi, J.J., and Yamazaki, H.o. (2008). Modeling and control of adhesion force in railway rolling stocks. *IEEE Control Systems Magazine*, 28(5), 44–58. doi:10.1109/MCS.2008.927334.
- Paynter, H.M. (1960). *Analysis and design of engineering systems*. M.I.T. Press, Cambridge, MA.
- Pichlik, P. and Zdenek, J. (2018). Locomotive Wheel Slip Control Method Based on an Unscented Kalman Filter. *IEEE Transactions on Vehicular Technology*, 67(7), 5730–5739. doi:10.1109/TVT.2018.2808379.
- Rochard, B.P. and Schmid, F. (2000). A review of methods to measure and calculate train resistances. *Proceedings of the Institution of Mechanical Engineers, Part F: Journal of Rail and Rapid Transit*, 214(4), 185–199. doi:10.1243/0954409001531306.
- Sadr, S., Khaburi, D.A., and Rodríguez, J. (2016). Predictive Slip Control for Electrical Trains. *IEEE Transactions on Industrial Electronics*, 63(6), 3446–3457. doi:10.1109/TIE.2016.2543180.
- Takaoka, Y. and Kawamura, A. (2000). Disturbance observer based adhesion control for Shinkansen. In *6th International Workshop on Advanced Motion Control. Proceedings (Cat. No.00TH8494)*, 169–174. doi:10.1109/AMC.2000.862851.
- Wu, Y., Wei, Z., Weng, J., and Deng, R.H. (2018). Position Manipulation Attacks to Balise-Based Train Automatic Stop Control. *IEEE Transactions on Vehicular Technology*, 67(6), 5287–5301. doi:10.1109/TVT.2018.2802444.
- Xiang, X., Qin, W., and Xiang, B. (2014). Research on a DSRC-Based Rear-End Collision Warning Model. *IEEE Transactions on Intelligent Transportation Systems*, 15(3), 1054–1065. doi:10.1109/TITS.2013.2293771.